Published in final edited form as:
Brain Res. 2011 January 31; 1371: 129–139. doi:10.1016/j.brainres.2010.10.088.

The Treatment of TBI with Human Marrow Stromal Cells Impregnated into Collagen Scaffold: Functional Outcome and Gene Expression Profile

Changsheng Qu, MD[1], **Asim Mahmood, MD**[1], **Xian Shuang Liu, MD**[2], **Ye Xiong, MD, PhD**[1], **Lei Wang, MD**[2], **Hongtao Wu, MD**[1], **Bo Li, MD, PhD**[1], **Zheng Gang Zhang, MD, PhD**[2], **David L. Kaplan, PhD**[3], and **Michael Chopp, PhD**[2,4]

[1] Department of Neurosurgery of Henry Ford Hospital, Detroit, Michigan

[2] Department of Neurology of Henry Ford Hospital, Detroit, Michigan

[3] Department of Biomedical Engineering, Tufts University, Medford, MA

[4] Department of Physics, Oakland University, Rochester, Michigan

Abstract

We have previously demonstrated that human marrow stromal cells (hMSCs) embedded in collagen I scaffolds significantly enhance the restorative therapeutic effect of hMSCs after traumatic brain injury (TBI). In this study, we test the hypothesis that the collagen scaffold alters gene expression in hMSCs and that hMSCs impregnated into scaffolds increase the astrocytic expression of vascular endothelial growth factor (VEGF) in the injured brain. Following TBI induced by controlled cortical impact injury, scaffold with hMSCs (3.0×10^6), hMSCs-only and saline were implanted into the lesion cavity one week after brain injury (n = 8/each group). Morris water Maze and modified neurological severity scores were performed to evaluate the spatial learning and sensorimotor functions, respectively. Lesion volume and expression of VEGF were measured one week after different treatments. In vitro, total RNA from hMSCs was extracted one week after culture with or without collagen I scaffold for evaluation of gene microarrays. Furthermore, an RT-PCR study on a select subgroup of genes was performed to identify the changes of expression between the culturing hMSCs with collagen scaffolds and hMSCs only. The treatment of TBI with collagen scaffold impregnated with hMSCs significantly decreases the functional deficits from TBI within 7 days after treatment, and significantly enhances the VEGF expression of astrocytes in the injured brain compared to the hMSCs-only group. In vitro data indicate that collagen scaffolds stimulate hMSCs to express multiple factors which may contribute to hMSC survival, tissue repair and functional recovery after TBI.

Keywords

endothelial vascular growth factor (VEGF); traumatic brain injury (TBI); marrow stromal cell; collagen scaffold; restorative therapy

1. Introduction

Traumatic brain injury (TBI) remains a major health problem worldwide. In the USA alone, the incidence of closed head injuries admitted annually to hospitals is 200 per 100,000

Send correspondence and reprint requests to: Asim Mahmood, MD, Department of Neurosurgery, Henry Ford Hospital, 2799 West Grand Blvd, Detroit, MI 48202, Phone: 313-916-1095 Fax: 313-916-7139, nsaam@neuro.hfh.edu.

(Narayan et al., 2002). Despite extensive research, no effective clinical treatment has been found to repair the biostructural damage resulting from TBI. Neurorestorative treatments for neural injury have taken essentially two paths, cellular and pharmacological (Mahmood et al., 2005). Cellular therapy has advantages over pharmacotherapy in that the interaction between exogenous cells and endogenous cells is dynamic and sensitive to the microenvironment (Chen et al., 2002). Marrow stromal cells (MSCs) have shown efficacy in improving functional outcome after TBI by direct intracerebral as well as systemic administration (Lu et al., 2001; Mahmood et al., 2001a; Mahmood et al., 2002; Mahmood et al., 2003; Mahmood et al., 2005; Mahmood et al., 2006). We have employed collagen scaffolds populated with human marrow stromal cells (hMSCs) to treat rats subjected to TBI and found reduction of lesion volume and improvement of functional outcome (Lu et al., 2007). However, the mechanism by which the scaffold augments functional recovery has not been investigated.

One of the major mechanisms by which hMSCs promote neural function is by induction of growth factors such as nerve growth factor (NGF), vascular endothelial growth factors (VEGFs) and brain-derived neurotrophic growth factor (BDNF) (Lu et al., 2002; Lu et al., 2004). hMSCs produce these growth factors and more importantly induce growth factors within parenchymal cells (Mahmood et al., 2004; Mahmood et al., 2005). Growth factors influence different aspects of neurogenesis, synaptogenesis and angiogenesis (Bibel and Barde, 2000; Huang and Reichardt, 2001; Palmer et al., 2000; Silverman et al., 1999). VEGF is an angiogenic factor and has multiple restorative effects (e.g. neurogenesis and axonal outgrowth) (Silverman et al., 1999; Sun et al., 2003). VEGF is a potent mitogen for endothelial cells and astrocytes, and promotes growth and survival of neurons (Silverman et al., 1999). In addition VEGF enhances neurogenesis in the adult brain, possibly via the establishment of a “vascular niche” that favors the proliferation and differentiation of neuronal precursors (Palmer et al., 2000; Silverman et al., 1999; Skold et al., 2005; Sun et al., 2010).

In the present study, we initially tested the functional changes both with the modified neurological severity score (mNSS) and Morris water maze (MWM) test. We then used immunohistochemistry to measure the expression of VEGF at one week after transplantation of hMSCs and scaffold + hMSCs in a rat TBI model. To test whether the gene expression profile is altered between hMSCs seeded into the scaffold and hMSCs-only in culture, we probed the interaction between hMSCs and scaffold in vitro using microarrays and real time polymerase chain reaction (RT-PCR).

2. Results

2.1 Neurological and sensorimotor functional responses

Injury in the left hemisphere cortex in rats caused neurological functional deficits as measured by mNSS. The higher the modified neurological severity score (mNSS), the worse the sensorimotor function. Figure 1 shows the changes of sensorimotor function in injured rats after different treatments. There was no significant difference in the mNSS scores among scaffold + hMSCs, hMSCs alone and the saline group on days 1, 4, and 7 after TBI. However, treatment with scaffold + hMSCs significantly deceased the mNSS score on day 14 (7 days after transplantation, $P < 0.0001$) compared to the hMSCs-alone and saline groups.

2.2 Spatial learning function changes

Spatial learning was tested during the last five days (days 10–14 post injury) using the MWM test without prior training before injury. TBI rats treated with scaffold + hMSCs

spent significantly more time in the correct quadrant than those treated with saline or hMSCs only on days 12 ($P = 0.016$ vs saline, $P = 0.02$ vs hMSC), 13 ($P = 0.04$ vs saline, $P = 0.004$ vs hMSC) and 14 ($P = 0.036$ vs saline, $P = 0.018$ vs hMSC) after TBI (Fig. 2). These data demonstrate that scaffold + hMSCs improve spatial learning function after TBI more effectively than do hMSCs-alone or saline.

2.3 scaffold + hMSCs treatment does not reduce the lesion volume

There was no significant difference in the lesion volume among the scaffold + hMSCs, hMSCs-only and saline groups (11.64 ± 1.09% for scaffold + hMSCs; 13.38 ± 2.67% for hMSCs only; 13.68 ± 2.77% for saline). These data indicate that the beneficial outcome from scaffold + hMSCs treatment derives from effects other than lesion reduction in this short-term study.

2.4 scaffold + hMSCs treatment increases hMSCs in the injured brain

Immunostaining with anti-human mitochondrial antibody (E5204) showed many hMSCs in the boundary zone of the scaffold + hMSCs group. However, very few hMSCs were visible in the hMSCs-only group (Fig. 3).

2.5 scaffold + hMSCs treatment increases VEGF expression in the injured brain

The expression of VEGF in astrocytes was detected with triple staining (VEGF, GFAP and DAPI, Fig. 4). Triple staining showed that a significantly higher density of astrocytes in the boundary zone were VEGF-positive in the scaffold + hMSCs group compared to the hMSCs-only group (for % of VEGF positive astrocytes, $P < 0.0001$ vs hMSCs; for the density of VEGF-positive astrocytes, $P = 0.00168$ vs hMSCs).

2.6 Collagen scaffolds induce hMSCs to upregulate the expression of functional genes

To test whether scaffolds induce gene expression in the cultured hMSCs, fold changes were recorded with the help of microarray analyses. A fold change of greater than 1.5 was shown by 129 genes and of these, 35 genes were involved in angiogenesis (Table 1), 41 upregulated genes were related to neurogenesis (Table 2), and 53 upregulated genes from the microarray were associated with signal transduction (Table 3).

To verify upregulated genes observed in microarrays, we performed real-time RT-PCR analysis on a small subgroup of selected genes (Table 4). The results showed that the fold changes in these genes are consistent with those of the microarray analyses (Figs. 5 and 6).

3. Discussion

No effective treatments are currently available for patients with TBI. Cell therapy is a promising restorative strategy which provides three-dimensional (3D) support to grafted cells, improving their survival, altering their properties and amplifying their therapeutic effect. The use of scaffold-based strategies in the regeneration of biological tissues requires the micro-architectural design of the scaffold to satisfy key microstructural and biological requirements (Li et al., 2006; Meinel et al., 2004; Meinel et al., 2005). Mechanically engineered hydrogel scaffolds are useful for promoting axonal regeneration, angiogenesis and functional recovery after spinal cord injury (Bakshi et al., 2004). The cell-scaffold interaction also increases the ability of the scaffold to support cell adhesion and proliferation, as well as promotes and guides 3D cell colonization by appropriately designing the microarchitectural features of the scaffold (Salerno et al., 2009). Our previous work demonstrated that collagen I scaffolds impregnated by hMSCs improve spatial learning and sensorimotor function, reduce the lesion volume, and foster the migration of hMSCs into the lesion boundary zone after TBI in rats (Lu et al., 2007). These studies

suggest that interactions are present between the scaffolds and the transplanted cells. However, hMSC-scaffold interaction has not been investigated.

Our present data revealed that culturing hMSCs with scaffolds caused upregulation of genes involved in angiogenesis (Table 1), neurogenesis (Table 2), and signal transduction (Table 3). Furthermore, further RT-PCR studies on a small subgroup of genes confirmed their enhanced expression in hMSCs cultured with collagen scaffolds (Table 4 and Fig. 6). The increased gene expression induced in hMSCs cultured with scaffolds may promote migration and survival of hMSCs in the injured brain and subsequent activation of neurorestorative mechanisms. Some of the scaffold-enhanced genes play prominent roles in neurorestoration and neuroprotection. For example, VEGF (fold change 6.8) enhances the proliferation and migration of neural progenitors in the subventricular zone and increases neurogenesis and maturation of newborn neurons in adult rat brain after stroke (Sun and Guo, 2005). VEGF expression is related to hippocampal activity and neurogenesis, and promotes learning and memory (Thau-Zuchman et al., 2010;Cao et al., 2004;During and Cao, 2006;Lee and Son, 2009;Pati et al., 2009). MSCs with VEGF overexpression produce effective myogenesis and host-derived angiogenesis, resulting in the prevention of progressive heart dysfunction after myocardial infarction (Gao et al., 2007). Our present study also shows that implanting hMSCs with scaffolds is more effective in inducing the expression of VEGF in astrocytes in the lesion boundary zone than implanting hMSCs alone. Increased parenchymal cell expression of VEGF by hMSCs with scaffold may contribute to enhanced angiogenesis after TBI (Qu et al., 2009;Xiong et al., 2009). Whether the increase in astrocytic expression of VEGF is secondary to scaffolds increasing the survival and concentration of donor hMSCs at the injury site, as shown by our data, or if the gene modification of hMSCs alters intercellular communication and thereby stimulates increased expression of VEGF in astrocytes, is unknown. Midkine (MDK; fold-change 5.27) is a heparin-binding growth factor involved in diverse biological phenomena, including neural survival, carcinogenesis, and tissue repair. It has a protective effect against ischemia/reperfusion injury in the heart and has cytoprotective activity in cultured neurons and tumor cells (Horiba et al., 2006) MSC over-expressing BCL-2 (fold-change 6.15) reduces MSC apoptosis, increases MSC survival, and enhances VEGF secretion under hypoxic conditions (Li et al., 2007). Survivin (fold-change 8.45), also called Baculoviral IAP repeat-containing 5 (BIRC5), a multifunctional protein essential for the completion of mitosis, can inhibit activated caspases, and has antiapoptotic properties (Kawamura et al., 2005). Lack of the endothelial cell surviving, causes embryonic defects in angiogenesis, cardiogenesis and neural tube closure (Zwerts et al., 2007). Survivin may be involved in regulation of neural cell proliferation after TBI (Johnson et al., 2004). Notch 4 (fold-change 7.00), a member of the Notch family of transmembrane receptors, is expressed primarily on endothelial cells and Notch 4 activation inhibits endothelial apoptosis (MacKenzie et al., 2004). Notch signaling regulates sprouting angiogenesis and coordinates the interaction between inflammation and angiogenesis under ischemic conditions (Al Haj Zen et al., 2010). Transforming growth factor-beta (TGF-beta) (fold-change 1.59), a family of growth factors with essential and multiple roles during embryonic development, regulates neuronal survival and death (Krieglstein et al., 2002). TGF-beta 2 provides neuroprotection on hydroxydopamine-induced neuronal death (Polazzi et al., 2009). The upregulation of many restorative and neuroprotective genes in hMSCs mediated by the collagen I scaffolds, may individually and in concert contribute to the improved neurological outcome. The present study was designed to elucidate the short-term effects of hMSCs-alone and scaffold + hMSCs treatment. Our data show that the lesion volume is not reduced after the short-term treatment, indicating that the improved functional outcome after scaffold + hMSCs treatment derives from effects other than direct lesion reduction. In the current experiment, collagen scaffolds stimulated the upregulation of many functional genes in hMSCs. These enhanced genes may contribute to angiogenesis, neurogenesis and signal transduction,

which in concert foster functional recovery. However, further investigation is warranted as to how scaffolds alter the genetic expression of seeded hMSCs.

In summary, we found that treatment with scaffold populated with hMSCs improves spatial learning and sensorimotor function in rats after TBI, which is consistent with our previous study (Lu et al., 2007). The scaffold with hMSCs promotes the expression of VEGF in astrocytes in the injured brain. In vitro study provides a data set for the first time comparing gene expression changes in the scaffold + hMSCs and hMSCs. Our data indicate that collagen scaffolds stimulate hMSCs to express multiple factors which may contribute to tissue repair and functional recovery after TBI.

4. Experimental procedures

All experimental procedures were approved by the Institutional Animal Care and Use Committee (IACUC) of Henry Ford Hospital.

4.1 Animal model

A controlled cortical impact (CCI) model of TBI in rats was used in the present study (Dixon et al., 1991; Mahmood et al., 2001b). Male Wistar rats weighing 300 to 350 g were anesthetized intraperitoneally with chloral hydrate (350 mg/kg body weight). Rectal temperature was maintained at 37°C by using a feedback-regulated water heating pad. A CCI device was used to induce injury. Rats were placed in a stereotactic frame. Two 10-mm-diameter craniotomies were performed adjacent to the central suture, midway between lambda and bregma. The second craniotomy allowed for lateral movement of cortical tissue. The dura mater was kept intact over the cortex. Injury was induced by impacting the left cortex (ipsilateral cortex) with a pneumatic piston containing a 6-mm-diameter tip at a rate of 4 m/second and 2.5 mm of compression. Velocity was measured with a linear velocity displacement transducer. Brain injury in this model is characterized by cystic cavity formation in cortex, which causes asymmetric neurological deficits (Lu et al., 2003) and selective cell damage in the hippocampal formation, causing spatial memory dysfunction (Lu et al., 2004). Therefore, sensorimotor and spatial memory tests were used to evaluate functional response to injury and treatment after TBI.

4.2 Experimental Groups

The experiment consists of two studies, in vivo and in vitro. In vivo, 24 adult male Wistar rats were randomly divided into three groups (n = 8/each group). All groups were initially subjected to TBI, and 7 days later received one of the following treatments: 1) scaffold + hMSCs; 2) hMSCs-only; and 3) saline. Rats in the first group were transplanted with scaffolds impregnated with hMSCs. hMSC-impregnated scaffolds (3×10^6 hMSCs per scaffold) were placed into the lesion cavity at one week after TBI. The second and third groups were treated with hMSCs only or saline injected into the lesion cavity, respectively, and at the same volume and time as the scaffold + hMSCs group. Spatial learning and motor-sensory functions were evaluated by the MWM test and mNSS, respectively. The rats were sacrificed seven days after transplantation. Brain samples from animals in the three groups were processed for immunohistochemical studies to evaluate lesion volume and morphological changes after different treatments.

In the in vitro study, the difference in gene expression was probed between hMSCs with or without collagen scaffold. One week after the culture, total RNA from hMSCs was extracted. The RNA was subsequently hybridized and genetic microarrays were performed. Furthermore, an RT-PCR study on a small subgroup of genes was performed to confirm the different changes of expression between the scaffold + hMSCs and hMSCs-only groups.

4.3 Sensorimotor functional test

The measurement of sensorimotor function was performed using mNSS (Chen et al., 2001; Lu et al., 2002; Sinz et al., 1999). This measurement was conducted on all rats before injury and on days 1, 4, 7 and 14 after TBI. The mNSS is a composite of motor (muscle status and abnormal movement), sensory (visual, tactile, and proprioceptive), beam balance, and reflex tests. Motor tests of the mNSS include seven items with a maximum score of 3 points, which mainly reflect the function of the motor representation area in the contralateral cortex. Damage to this area causes contralateral limb paralysis, leading to high scores on the mNSS motor tests. Sensory tests include two items with a maximum score of 2, reflecting a combination of visual, tactile, and deep sensations. A unilateral lesion in the sensory and motor representations of the forelimb in the somatosensory cortex can produce contralateral asymmetry (Day and Schallert, 1996; Day et al., 1999; Yamada et al., 1999). The placing test, included as a sensory test of the mNSS, also reflects an aspect of motor function, because the corticospinal pathway mediates the execution of the placing reaction and lesions in this region produce an enduring forelimb-placing deficit (Reh and Kalil, 1982). Beam balance tests (part of the asymmetry test) contain seven items with a maximum score of 6, mainly reflecting hindlimb placing performance, which is controlled by the contralateral cortical representation of motor function. Damage to this area causes dragging of the contralateral hindlimb (the hindlimb is not placed on the beam), or the hindlimb is placed on the vertical surface of the beam to help support the animal's weight and to aid in maintaining balance, which reflects a high score on the beam balance tests. The last part of the mNSS includes the pinna, corneal and startle reflexes, and abnormal movements. In this model, injury in the left hemisphere of the cortex in rats causes sensory and motor functional deficits with elevated scores on motor, sensory, and beam balance tests in the early phase after injury (day 1 post injury) (Lu et al., 2003) Absent reflexes and abnormal movements are present in rats with severe injury.

4.4 Spatial learning Memory test

Our spatial memory testing procedure is a modification of the Morris water maze test, as described previously (Day and Schallert, 1996; Day et al., 1999; Lu et al., 2004; Yamada et al., 1999). Data collection was automated using the HVS Image 2020 Plus Tracking System (US HVS Image, San Diego, CA). The rats were tested on days 10–14 after TBI. At the start of a trial, the rat was randomly placed at one of four fixed starting points, randomly facing toward the wall (designated north, south, east, and west), and was allowed to swim for 90 sec or until it found the platform. The platform was located in a randomly changing position within the northeast quadrant throughout the test period (for example, sometimes equidistant from the center and edge of the pool, against the wall, near the center of the pool, or at the edges of the northeast quadrant). If the animal was unable to find the platform within 90 sec, the experiment was terminated and a maximal score of 90 sec was assigned. The percentage of time traveled within the northeast (correct) quadrant was calculated relative to the total amount of time spent swimming before reaching the platform.

4.5 Tissue Preparation

In the in vivo study rats from scaffold + hMSCs, hMSCs-only and saline-treated groups were anesthetized intraperitoneally with ketamine and xylazine and perfused transcardially with saline solution containing heparin 14 days after TBI. After saline perfusion, the animals were perfused with 4% paraformaldehyde in 0.1 M PBS (pH 7.4). The brains were removed, postfixed in 10% formalin for 1 to 2 days at room temperature, and then processed for paraffin sectioning. A series of 6-μm-thick tissue sections were cut using a microtome through each of seven standard blocks. A section from every block was stained with H & E for lesion volume calculation. The indirect lesion area was calculated (that is, the intact area of the ipsilateral hemisphere is subtracted from the area of the contralateral hemisphere)

(Swanson et al., 1990) and the lesion volume presented as a volume percentage of the lesion compared with the contralateral hemisphere.

4.6 Immunohistochemistry staining

To identify the transplanted hMSCs, brain tissue sections, after being deparaffinized and boiled in 1% citric acid buffer (pH 6), were incubated in 1% bovine serum albumin/PBS at room temperature for 30 min and subsequently were treated with mouse anti–human mitochondrial antibody (Dako Cytomation, Carpinteria, CA) diluted to 1:200 in PBS at 4°C overnight. Following sequential incubation with biotin-conjugated anti–mouse immunoglobulin G (dilution 1:100; Dakopatts, Carpinteria, CA), the sections were treated with an avidin-biotin-peroxidase system (ABC kit; Vector Laboratories, Inc., Burlingame, CA). Diaminobenzidine was then used as a sensitive chromogen for light microscopy.

To examine the expression of VEGF vascular endothelial growth factor in injured brain, a Polyclonal IgG anti-VEGF antibody (Santa Cruz Biotechnology, Santa Cruz, CA) at a titer of 1: 400 was used to incubate the slide in 4 °C overnight. The secondary antibody (Cy3, 1:200 in PBS Jackson ImmunoResearch, West Grove, PA) was followed. Each of the aforementioned steps was followed by four 5-min rinses in PBS. Rabbit anti-glial fibrillary acidic protein was used to detected astrocytes in injured brain. The second antibody (FITC, 1:200 in PBS, Jackson ImmunoResearch, West Grove, PA) was added in room temperature for 30 min. The sections were counterstained with 4′, 6-diamidino-2-phenyl-indole, dihydrochloride for the identification of nuclei.

4.7 Seeding hMSCs on scaffolds and transplantation

Ultrafoam scaffolds, collagen type 1 were obtained from commercial sources (Davol, R1, and USA). Scaffolds were pre-wet in culture medium consisting of Dulbecco's modified Eagle's medium (DMEM) supplemented with 10% fetal calf serum (FCS), 100 U/ml penicillin, 100 μg/ml streptomycin, 0.1 mM nonessential amino acids and 1 ng/ml of basic fibroblast growth factor (bFGF) (Life Technologies, Rockville, MD). Medium was aspirated and scaffolds were washed with PBS one time and then aseptically transferred using tweezers (1 scaffold per tube) to a 50-ml sterile centrifuge tube allowing the scaffolds to sit at the bottom of the tube. Following trypsinization of hMSCs from ex vivo expansion conditions, hMSCs were resuspended thoroughly and transferred gently (3×10^6 hMSCs per scaffold) into 200 μl of culture medium. 100 μl of culture medium was then applied two times successively to opposite sides of the body of the cylindrical scaffold. The scaffold and cell solution was incubated for 30 min in a humidified incubator to facilitate primary cell seeding. During this time the scaffolds were gently agitated within the solution manually twice every 15 min. Following primary seeding, the centrifuge tubes were filled with an additional 3 ml of culture medium and then scaffolds populated with hMSCs were incubated in 37 °C overnight (Qu et al., 2009). On the following day, the scaffold with hMSCs was implanted into the lesion cavity on the seventh days after TBI. The group of animals treated with hMSCs alone was injected with hMSCs in solution into the lesion cavity under the same conditions (Xiong et al., 2009). The control group animals were treated with saline. The animals were sacrificed 14 days after TBI. For the in vitro study, the scaffolds with 3×10^6 hMSCs were transferred into three new plates and cultured for one week. Serving as control in a group, 3×10^6 hMSCs in three plates were cultured in the same incubator (37°C, 5% CO_2).

4.8 RNA isolation and gene expression microarray

Total RNAs from cultures were extracted using an RNeasy spin column purification kit (Qiagen Valencia, CA, USA) (Liu et al., 2007). The non-radioactive oligo GEArrays PAHS-404, OHS-024 and OHS-014 (SABiosciences, Frederick, MD) were used, and

hybridization procedures were performed according to the manufacturer's instructions. The biotin UTP-labeled oligo probes were specifically generated in the presence of a designed set of gene-specific primers. Chemiluminescent detection steps were performed by subsequent incubation of the filters with alkaline phosphatase-conjugated streptavidin and CDP-Star substrate (SABiosciences).

4.9 Reverse transcription and quantitative Real-time RT-PCR

Total RNAs isolated from hMSCs alone or hMSCs seeded into scaffolds (n = 3) were processed by reverse-transcription Real-time PCR performed in ABI Prism 7700 Sequence Detection Wustem (Applied Biosystems, Foster City, CA) by using SYBR Green PCR Master Mix (Applied Biosystems) with three-stage program parameters provided by the manufacturer (Wang et al., 2004). Table 1 lists the primers (Invitrogen Corporation, Carlsbad, CA) examined in the present study. Each sample was tested in triplicate and data obtained from three independent experiments were expressed as a subtraction of the quantity of specific transcriptions to the quantity of the control gene (β-actin) in mean arbitrary units. CT values were quantified by the $2^{-\Delta\Delta Ct}$ method (Livak and Schmittgen, 2001).

4.10 Data processing

For quantification, the intensity of spots was measured using GEArray Expression Analysis Suite software (SABiosciences). To reduce the contamination by adjacent spots, "clover on" mode was used, which considers the four individual spots as a form of border for the capture of expression data. Total density was divided by the number of pixels to obtain average intensities that were used to compare gene expression levels between the hMSC-only group and the scaffolds populated with hMSCs group (Liu et al., 2007).

4.11 Statistical analysis

All data are presented as the mean ± standard deviation (SD). For modified neurological severity score and water maze test, a one way ANOVA followed by post hoc Student-Newman-Keuls (SNK) test were used to compare the difference between the scaffold + hMSCs, hMSCs alone and saline-treated groups (Lu M et al., 2003). Student t-test was used to consider the difference in the percentage and density of positive VEGF astrocytes in the ipsilateral hemisphere between the scaffold-hMSCs treated group and hMSCs alone. Statistical significance was set at $P < 0.05$. All measures were analyzed by observers blinded to individual treatments.

Acknowledgments

This research was supported by National Institutes of Health grants PO1 NS42345, RO1 NS042259 and P41 EB002520

Special thanks to Susan MacPhee-Gray for editorial assistance and Cynthia Roberts for pathology assistance.

References

Al Haj Zen A, Oikawa A, Bazan-Peregrino M, Meloni M, Emanueli C, Madeddu P. Inhibition of delta-like-4-mediated signaling impairs reparative angiogenesis after ischemia. Circ Res. 2010; 107:283–293. [PubMed: 20508179]

Bakshi A, Fisher O, Dagci T, Himes BT, Fischer I, Lowman A. Mechanically engineered hydrogel scaffolds for axonal growth and angiogenesis after transplantation in spinal cord injury. J Neurosurg Spine. 2004; 1:322–329. [PubMed: 15478371]

Bibel M, Barde YA. Neurotrophins: key regulators of cell fate and cell shape in the vertebrate nervous system. Genes Dev. 2000; 14:2919–2937. [PubMed: 11114882]

Cao L, Jiao X, Zuzga DS, Liu Y, Fong DM, Young D, During MJ. VEGF links hippocampal activity with neurogenesis, learning and memory. Nat Genet. 2004; 36:827–835. [PubMed: 15258583]

Chen J, Li Y, Wang L, Zhang Z, Lu D, Lu M, Chopp M. Therapeutic benefit of intravenous administration of bone marrow stromal cells after cerebral ischemia in rats. Stroke. 2001; 32:1005–1011. [PubMed: 11283404]

Chen X, Katakowski M, Li Y, Lu D, Wang L, Zhang L, Chen J, Xu Y, Gautam S, Mahmood A, Chopp M. Human bone marrow stromal cell cultures conditioned by traumatic brain tissue extracts: growth factor production. J Neurosci Res. 2002; 69:687–691. [PubMed: 12210835]

Day LB, Schallert T. Anticholinergic effects on acquisition of place learning in the Morris water task: spatial mapping deficit or inability to inhibit nonplace strategies? Behav Neurosci. 1996; 110:998–1005. [PubMed: 8919002]

Day LB, Weisand M, Sutherland RJ, Schallert T. The hippocampus is not necessary for a place response but may be necessary for pliancy. Behav Neurosci. 1999; 113:914–924. [PubMed: 10571475]

Dixon CE, Clifton GL, Lighthall JW, Yaghmai AA, Hayes RL. A controlled cortical impact model of traumatic brain injury in the rat. J Neurosci Methods. 1991; 39:253–262. [PubMed: 1787745]

During MJ, Cao L. VEGF, a mediator of the effect of experience on hippocampal neurogenesis. Curr Alzheimer Res. 2006; 3:29–33. [PubMed: 16472200]

Gao F, He T, Wang H, Yu S, Yi D, Liu W, Cai Z. A promising strategy for the treatment of ischemic heart disease: Mesenchymal stem cell-mediated vascular endothelial growth factor gene transfer in rats. Can J Cardiol. 2007; 23:891–898. [PubMed: 17876381]

Horiba M, Kadomatsu K, Yasui K, Lee JK, Takenaka H, Sumida A, Kamiya K, Chen S, Sakuma S, Muramatsu T, Kodama I. Midkine plays a protective role against cardiac ischemia/reperfusion injury through a reduction of apoptotic reaction. Circulation. 2006; 114:1713–1720. [PubMed: 17015789]

Huang EJ, Reichardt LF. Neurotrophins: roles in neuronal development and function. Annu Rev Neurosci. 2001; 24:677–736. [PubMed: 11520916]

Johnson EA, Svetlov SI, Pike BR, Tolentino PJ, Shaw G, Wang KK, Hayes RL, Pineda JA. Cell-specific upregulation of survivin after experimental traumatic brain injury in rats. J Neurotrauma. 2004; 21:1183–1195. [PubMed: 15453988]

Kawamura K, Fukuda J, Shimizu Y, Kodama H, Tanaka T. Survivin contributes to the anti-apoptotic activities of transforming growth factor alpha in mouse blastocysts through phosphatidylinositol 3′-kinase pathway. Biol Reprod. 2005; 73:1094–1101. [PubMed: 16079309]

Krieglstein K, Strelau J, Schober A, Sullivan A, Unsicker K. TGF-beta and the regulation of neuron survival and death. J Physiol Paris. 2002; 96:25–30. [PubMed: 11755780]

Lee E, Son H. Adult hippocampal neurogenesis and related neurotrophic factors. BMB Rep. 2009; 42:239–244. [PubMed: 19470236]

Li C, Vepari C, Jin HJ, Kim HJ, Kaplan DL. Electrospun silk-BMP-2 scaffolds for bone tissue engineering. Biomaterials. 2006; 27:3115–3124. [PubMed: 16458961]

Li W, Ma N, Ong LL, Nesselmann C, Klopsch C, Ladilov Y, Furlani D, Piechaczek C, Moebius JM, Lutzow K, Lendlein A, Stamm C, Li RK, Steinhoff G. Bcl-2 engineered MSCs inhibited apoptosis and improved heart function. Stem Cells. 2007; 25:2118–2127. [PubMed: 17478584]

Liu XS, Zhang ZG, Zhang RL, Gregg S, Morris DC, Wang Y, Chopp M. Stroke induces gene profile changes associated with neurogenesis and angiogenesis in adult subventricular zone progenitor cells. J Cereb Blood Flow Metab. 2007; 27:564–574. [PubMed: 16835628]

Livak KJ, Schmittgen TD. Analysis of relative gene expression data using real-time quantitative PCR and the 2(−Delta Delta C(T)) method. Methods. 2001; 25:402–408. [PubMed: 11846609]

Lu D, Mahmood A, Wang L, Li Y, Lu M, Chopp M. Adult bone marrow stromal cells administered intravenously to rats after traumatic brain injury migrate into brain and improve neurological outcome. Neuroreport. 2001; 12:559–563. [PubMed: 11234763]

Lu D, Li Y, Mahmood A, Wang L, Rafiq T, Chopp M. Neural and marrow-derived stromal cell sphere transplantation in a rat model of traumatic brain injury. J Neurosurg. 2002; 97:935–940. [PubMed: 12405384]

Lu D, Mahmood A, Zhang R, Copp M. Upregulation of neurogenesis and reduction in functional deficits following administration of DEtA/NONOate, a nitric oxide donor, after traumatic brain injury in rats. J Neurosurg. 2003; 99:351–361. [PubMed: 12924710]

Lu D, Goussev A, Chen J, Pannu P, Li Y, Mahmood A, Chopp M. Atorvastatin reduces neurological deficit and increases synaptogenesis, angiogenesis, and neuronal survival in rats subjected to traumatic brain injury. J Neurotrauma. 2004; 21:21–32. [PubMed: 14987462]

Lu D, Mahmood A, Qu C, Hong X, Kaplan D, Chopp M. Collagen scaffolds populated with human marrow stromal cells reduce lesion volume and improve functional outcome after traumatic brain injury. Neurosurgery. 2007; 61:596–602. discussion 602–603. [PubMed: 17881974]

Lu M, Chen J, Lu D, Yi L, Mahmood A, Chopp M. Global test statistics for treatment effect of stroke and traumatic brain injury in rats with administration of bone marrow stromal cells. J Neurosci Methods. 2003b; 128:183–190. [PubMed: 12948561]

MacKenzie F, Duriez P, Wong F, Noseda M, Karsan A. Notch4 inhibits endothelial apoptosis via RBP-Jkappa-dependent and -independent pathways. J Biol Chem. 2004; 279:11657–11663. [PubMed: 14701863]

Mahmood A, Lu D, Wang L, Li Y, Lu M, Chopp M. Treatment of traumatic brain injury in female rats with intravenous administration of bone marrow stromal cells. Neurosurgery. 2001a; 49:1196–1203. discussion 1203–1204. [PubMed: 11846913]

Mahmood A, Lu D, Yi L, Chen JL, Chopp M. Intracranial bone marrow transplantation after traumatic brain injury improving functional outcome in adult rats. J Neurosurg. 2001b; 94:589–595. [PubMed: 11302657]

Mahmood A, Lu D, Wang L, Chopp M. Intracerebral transplantation of marrow stromal cells cultured with neurotrophic factors promotes functional recovery in adult rats subjected to traumatic brain injury. J Neurotrauma. 2002; 19:1609–1617. [PubMed: 12542861]

Mahmood A, Lu D, Lu M, Chopp M. Treatment of traumatic brain injury in adult rats with intravenous administration of human bone marrow stromal cells. Neurosurgery. 2003; 53:697–702. discussion 702–703. [PubMed: 12943585]

Mahmood A, Lu D, Chopp M. Intravenous administration of marrow stromal cells (MSCs) increases the expression of growth factors in rat brain after traumatic brain injury. J Neurotrauma. 2004; 21:33–39. [PubMed: 14987463]

Mahmood A, Lu D, Qu C, Goussev A, Chopp M. Human marrow stromal cell treatment provides long-lasting benefit after traumatic brain injury in rats. Neurosurgery. 2005; 57:1026–1031. [PubMed: 16284572]

Mahmood A, Lu D, Qu C, Goussev A, Chopp M. Long-term recovery after bone marrow stromal cell treatment of traumatic brain injury in rats. J Neurosurg. 2006; 104:272–277. [PubMed: 16509501]

Meinel L, Hofmann S, Karageorgiou V, Zichner L, Langer R, Kaplan D, Vunjak-Novakovic G. Engineering cartilage-like tissue using human mesenchymal stem cells and silk protein scaffolds. Biotechnol Bioeng. 2004; 88:379–391. [PubMed: 15486944]

Meinel L, Fajardo R, Hofmann S, Langer R, Chen J, Snyder B, Vunjak-Novakovic G, Kaplan D. Silk implants for the healing of critical size bone defects. Bone. 2005; 37:688–698. [PubMed: 16140599]

Narayan RK, Michel ME, Ansell B, Baethmann A, Biegon A, Bracken MB, Bullock MR, Choi SC, Clifton GL, Contant CF, Coplin WM, Dietrich WD, Ghajar J, Grady SM, Grossman RG, Hall ED, Heetderks W, Hovda DA, Jallo J, Katz RL, Knoller N, Kochanek PM, Maas AI, Majde J, Marion DW, Marmarou A, Marshall LF, McIntosh TK, Miller E, Mohberg N, Muizelaar JP, Pitts LH, Quinn P, Riesenfeld G, Robertson CS, Strauss KI, Teasdale G, Temkin N, Tuma R, Wade C, Walker MD, Weinrich M, Whyte J, Wilberger J, Young AB, Yurkewicz L. Clinical trials in head injury. J Neurotrauma. 2002; 19:503–557. [PubMed: 12042091]

Palmer TD, Willhoite AR, Gage FH. Vascular niche for adult hippocampal neurogenesis. J Comp Neurol. 2000; 425:479–494. [PubMed: 10975875]

Pati S, Orsi SA, Moore AN, Dash PK. Intra-hippocampal administration of the VEGF receptor blocker PTK787/ZK222584 impairs long-term memory. Brain Res. 2009; 1256:85–91. [PubMed: 19100245]

Polazzi E, Altamira LE, Eleuteri S, Barbaro R, Casadio C, Contestabile A, Monti B. Neuroprotection of microglial conditioned medium on 6-hydroxydopamine-induced neuronal death: role of transforming growth factor beta-2. J Neurochem. 2009; 110:545–556. [PubMed: 19457129]

Qu C, Xiong Y, Mahmood A, Kaplan DL, Goussev A, Ning R, Chopp M. Treatment of traumatic brain injury in mice with bone marrow stromal cell-impregnated collagen scaffolds. J Neurosurg. 2009; 111:658–665. [PubMed: 19425888]

Reh T, Kalil K. Functional role of regrowing pyramidal tract fibers. J Comp Neurol. 1982; 211:276–283. [PubMed: 6294149]

Salerno A, Oliviero M, Di Maio E, Iannace S, Netti PA. Design of porous polymeric scaffolds by gas foaming of heterogeneous blends. J Mater Sci Mater Med. 2009; 20:2043–2051. [PubMed: 19430895]

Silverman WF, Krum JM, Mani N, Rosenstein JM. Vascular, glial and neuronal effects of vascular endothelial growth factor in mesencephalic explant cultures. Neuroscience. 1999; 90:1529–1541. [PubMed: 10338318]

Sinz EH, Kochanek PM, Dixon CE, Clark RS, Carcillo JA, Schiding JK, Chen M, Wisniewski SR, Carlos TM, Williams D, DeKosky ST, Watkins SC, Marion DW, Billiar TR. Inducible nitric oxide synthase is an endogenous neuroprotectant after traumatic brain injury in rats and mice. J Clin Invest. 1999; 104:647–656. [PubMed: 10487779]

Skold MK, von Gertten C, Sandberg-Nordqvist AC, Mathiesen T, Holmin S. VEGF and VEGF receptor expression after experimental brain contusion in rat. J Neurotrauma. 2005; 22:353–367. [PubMed: 15785231]

Sun FY, Guo X. Molecular and cellular mechanisms of neuroprotection by vascular endothelial growth factor. J Neurosci Res. 2005; 79:180–184. [PubMed: 15573409]

Sun J, Sha B, Zhou W, Yang Y. VEGF-mediated angiogenesis stimulates neural stem cell proliferation and differentiation in the premature brain. Biochem Biophys Res Commun. 2010; 394:146–152. [PubMed: 20188072]

Sun Y, Jin K, Xie L, Childs J, Mao XO, Logvinova A, Greenberg DA. VEGF-induced neuroprotection, neurogenesis, and angiogenesis after focal cerebral ischemia. J Clin Invest. 2003; 111:1843–1851. [PubMed: 12813020]

Swanson RA, Morton MT, Tsao-Wu G, Savalos RA, Davidson C, Sharp FR. A semiautomated method for measuring brain infarct volume. J Cereb Blood Flow Metab. 1990; 10:290–293. [PubMed: 1689322]

Thau-Zuchman O, Shohami E, Alexandrovich AG, Leker RR. Vascular endothelial growth factor increases neurogenesis after traumatic brain injury. J Cereb Blood Flow Metab. 2010; 30:1008–1016. [PubMed: 20068579]

Wang L, Zhang Z, Zhang R, Hafner MS, Wong HK, Jiao Z, Chopp M. Erythropoietin up-regulates SOCS2 in neuronal progenitor cells derived from SVZ of adult rat. Neuroreport. 2004; 15:1225–1229. [PubMed: 15167538]

Xiong Y, Qu C, Mahmood A, Liu Z, Ning R, Li Y, Kaplan DL, Schallert T, Chopp M. Delayed transplantation of human marrow stromal cell-seeded scaffolds increases transcallosal neural fiber length, angiogenesis, and hippocampal neuronal survival and improves functional outcome after traumatic brain injury in rats. Brain Res. 2009; 1263:183–191. [PubMed: 19368838]

Yamada K, Tanaka T, Mamiya T, Shiotani T, Kameyama T, Nabeshima T. Improvement by nefiracetam of beta-amyloid-(1–42)-induced learning and memory impairments in rats. Br J Pharmacol. 1999; 126:235–244. [PubMed: 10051141]

Zwerts F, Lupu F, De Vriese A, Pollefeyt S, Moons L, Altura RA, Jiang Y, Maxwell PH, Hill P, Oh H, Rieker C, Collen D, Conway SJ, Conway EM. Lack of endothelial cell survivin causes embryonic defects in angiogenesis, cardiogenesis, and neural tube closure. Blood. 2007; 109:4742–4752. [PubMed: 17299096]

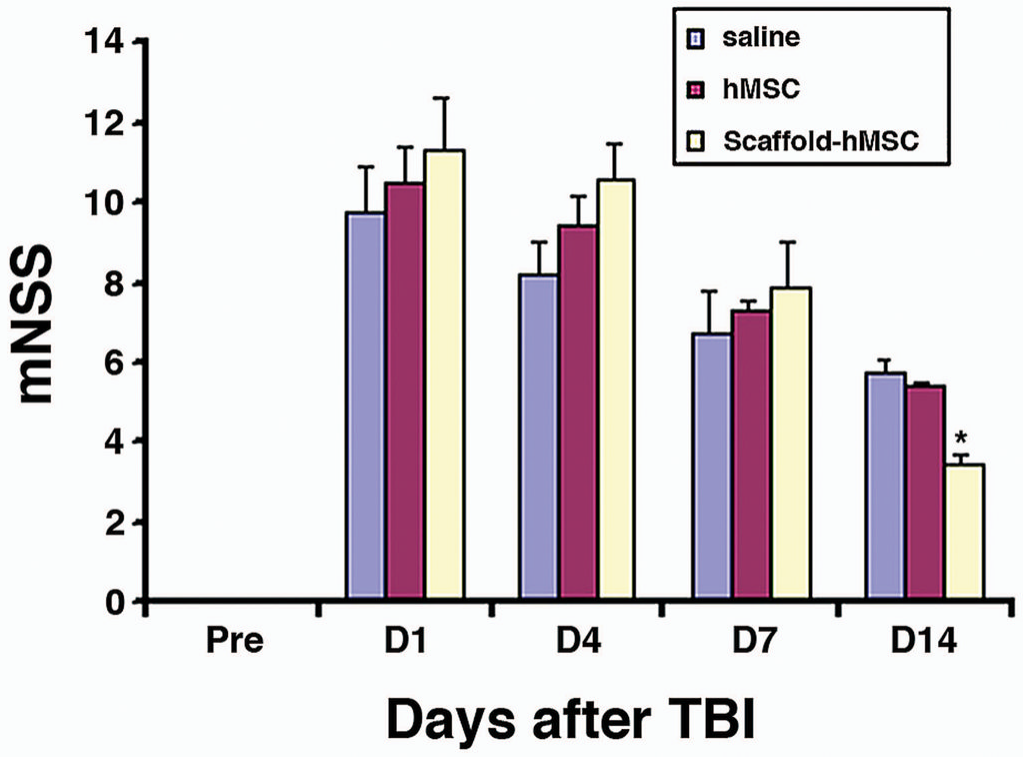

Fig. 1.

Functional improvement detected on the modified Neurological Severity Scores (mNSS). The scaffold + hMSCs group showed a significant functional improvement on day 14 after TBI, compared with the saline (*$P < 0.0001$) and the hMSCs-treated (*$P < 0.0001$) groups. Data are presented as the mean ± SD (n = 8/group).

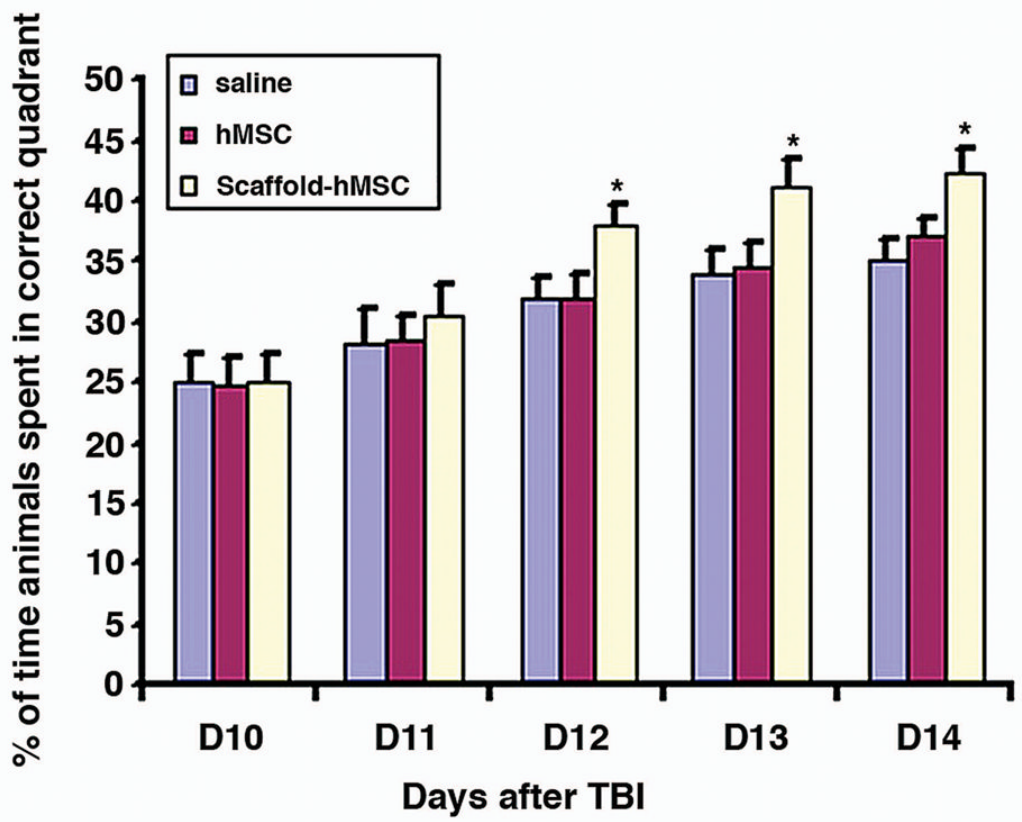

Fig. 2.

This figure shows the spatial learning function after different treatments. The scaffold + hMSCs treated group had a significant functional improvement from day 12 to day 14 after TBI, compared to saline and hMSCs-treated groups (day 12, $P = 0.016$ vs saline, $P = 0.02$ vs hMSC; day 13, $P = 0.04$ vs saline, $P = 0.004$ vs hMSC; day 14, $P = 0.036$ vs saline, $P = 0.018$ vs hMSC). Data are presented as the mean ± SD (n = 8/group).

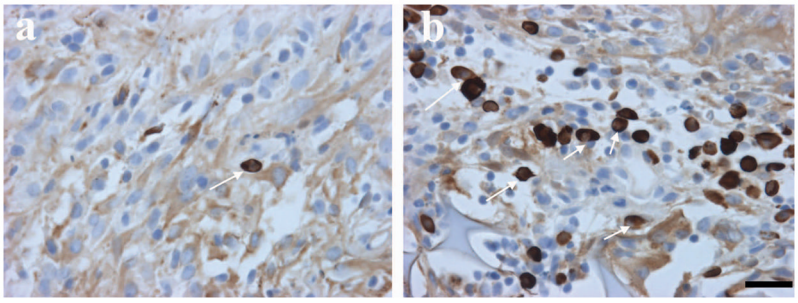

Fig. 3.

Immunostaining shows hMSCs (brown) in the lesion boundary zone: a. There are very few positive hMSCs visible in the hMSCs-alone treatment group. b. The figure shows many hMSCs in the scaffold +hMSCs treatment group. Scale bar shown in b = 25 μm.

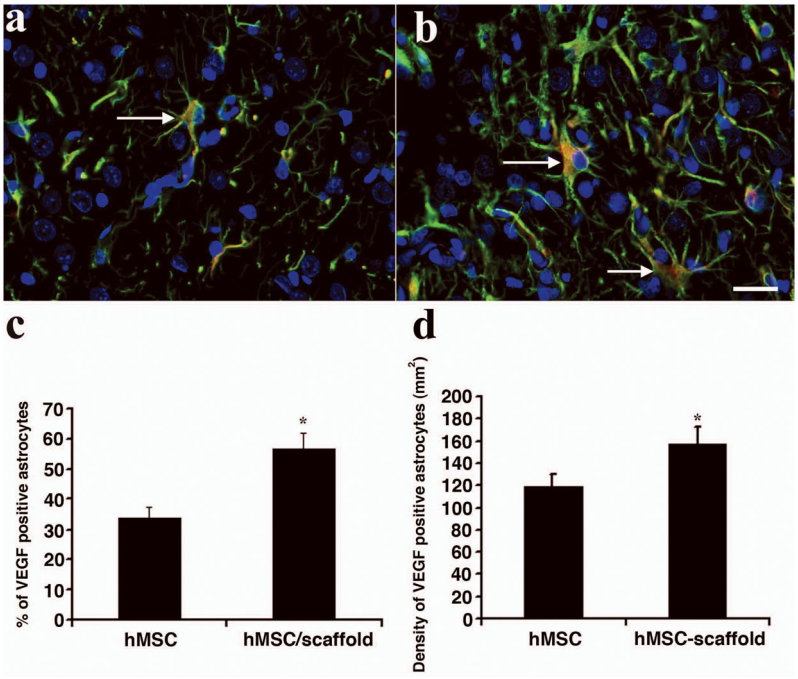

Fig. 4.

Triple immunostaining shows the expression of VEGF in astrocytes in the injured area. a. hMSCs-only group. b. scaffold + hMSCs treated group. c. Percentage of VEGF-positive astrocytes. d. Density of VEGF-positive astrocytes. Scale bar in b = 25μm. The bar graph C shows that scaffold + hMSCs treatment increases the percentage of VEGF-positive astrocytes compared to hMSCs-alone treatment (*$P < 0.05$, n = 8/group). The bar graph D shows that the treatment with scaffold + hMSCs increases the density of VEGF-positive astrocytes in the injured brain, compared to that of the hMSCs-only group (*$P < 0.05$ n = 8/group).

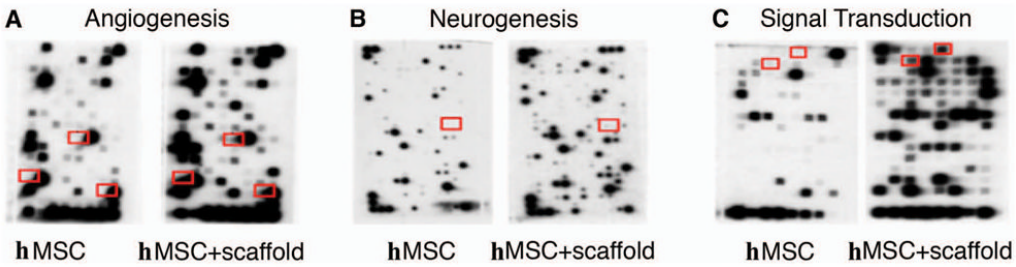

Fig. 5.

Panel A shows NOTCH4, VEGFA, and TGFB2 genes in red boxes based on the results of microarray analysis from hMSCs and scaffold + hMSCs in 7-day culture by means of the non-radioactive GEArray Q series cDNA expression array filters. Panels B and C show separately that the upregulated-genes MDK, BCL2 and BIRC5, exist only in the difference in microarray results between the hMSCs-only and scaffold + hMSCs groups.

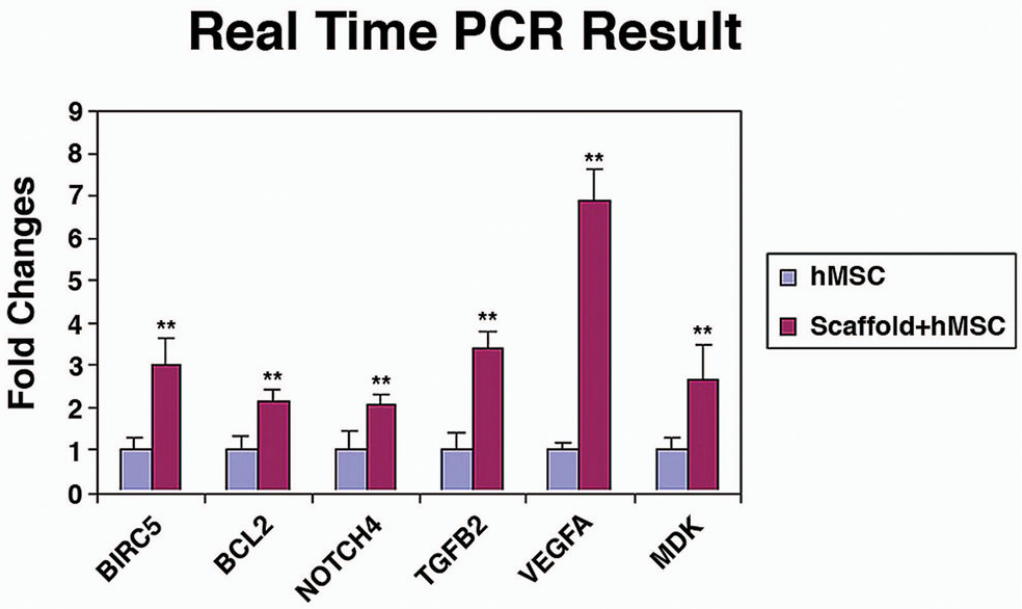

Fig. 6.

Bar graph showing RT-PCR analyses confirming that selective upregulated genes detected on the microarrays (i.e., VEGFA, TGFB2, NOTCH4, MDK, BCL2, and BIRC5), shows a significant difference between scaffold + hMSCs and hMSCs-only. * $P < 0.05$ (n = 3).

Table 1

Gene expression alteration of hMSCs in scaffold (angiogenesis)

Symbol	Gene name	Ref Seq Number	Fold change
ANGPTL3	Angiopoietin-like 3	NM_014495	9.36
ANGPTL4	Angiopoietin-like 4	NM_001039667	8.92
NOTCH4	Notch homolog 4 (Drosophila)	NM_004557	7.00
VEGFA	Vascular endothelial growth factor A	NM_003376	6.81
EFNA1	Ephrin-A1	NM_182685	6.32
ID1	Inhibitor of DNA binding 1,	NM_002165	5.59
TGFB2	Transforming growth factor, beta 2	NM_003238	5.34
HGF	Hepatocyte growth factor (hepapoietin A; scatter factor)	NM_000601	5.30
CSF3	Colony stimulating factor 3 (granulocyte)	NM_000759	5.20
EFNA5	Ephrin-A5	NM_001962	4.58
IL18	Interleukin 18 (interferon-gamma-inducing factor)	NM_001562	3.75
TIE1	Tyrosine kinase with immunoglobulin-like and EGF-like domains 1	NM_005424	3.70
EPAS1	Endothelial PAS domain protein 1	NM_001430	3.39
TEK	TEK tyrosine kinase, endothelial	NM_000459	3.17
SPHK1	Sphingosine kinase 1	NM_021972	3.05
LECT1	Leukocyte cell derived chemotaxin 1	NM_007015	2.96
NRP1	Neuropilin 1	NM_003873	2.78
CXCL6	Chemokine (C-X-C motif) ligand 6	NM_002993	2.69
TIMP1	TIMP metallopeptidase inhibitor 1	NM_003254	2.64
KDR	Kinase insert domain receptor	NM_002253	2.62
IL8	Interleukin 8	NM_000584	2.53
CXCL3	Chemokine (C-X-C motif) ligand 3	NM_002090	2.38
NPR1	Natriuretic peptide receptor A/guanylate cyclase A	NM_000906	2.28
FGF1	Fibroblast growth factor 1 (acidic)	NM_000800	2.17
MMP9	Matrix metallopeptidase 9	NM_004994	2.07
HPSE	Heparanase	NM_006665	2.02
THBS1	Thrombospondin 1	NM_003246	1.94
IL10	Interleukin 10	NM_000572	1.85
PGF	Placental growth factor	NM_002632	1.77
IFNG	Interferon, gamma	NM_000619	1.66
JAG1	Jagged 1 (Alagille syndrome)	NM_000214	1.60
TGFB1	Transforming growth factor, beta 1	NM_000660	1.59
CXCL11	Chemokine (C-X-C motif) ligand 11	NM_005409	1.57
CXCL2	Chemokine (C-X-C motif) ligand 2	NM_002089	1.56
EREG	Epiregulin	NM_001432	1.53

Table 2

Gene expression alteration of hMSCs in scaffolds (neurogenesis)

Symbol	Genes name	Ref Seq Number	Fold change
MDK	Midkine (neurite growth-promoting factor 2)	NM_002391	5.27
SHOX2	Short stature homeobox 2	NM_003030	5.04
SPG7	Spastic paraplegia 7, paraplegin	NM_003119	4.25
RAPGEFL1	Rap guanine nucleotide exchange factor (GEF)-like 1	NM_016339	4.05
LARGE	Like-glycosyltransferase	NM_004737	3.50
GPI	Glucose phosphate isomerase	NM_000175	3.42
PBX3	Pre-B-cell leukemia homeobox 3	NM_006195	3.22
MAFB	V-maf musculoaponeurotic fibrosarcoma oncogene homolog B	NM_005461	3.20
REG1B	Regenerating islet-derived 1 beta	NM_006507	3.00
ACHE	Acetylcholinesterase (YT blood group)	NM_000665	2.93
PBX1	Pre-B-cell leukemia homeobox 1	NM_002585	2.92
MBNL1	Muscleblind-like (Drosophila)	NM_021038	2.80
MLL	Myeloid/lymphoid or mixed-lineage leukemia	NM_005933	2.68
SOX11	SRY (sex determining region Y)-box 11	NM_003108	2.67
NGFR	Nerve growth factor receptor (TNFR superfamily, member 16)	NM_002507	2.62
BMP1	Bone morphogenetic protein 1	NM_006129	2.55
DBN1	Drebrin 1	NM_004395	2.53
HDAC4	Histone deacetylase 4	NM_006037	2.51
NOTCH2NL	Notch homolog 2 (Drosophila) N-terminal like	NM_203458	2.48
LIMK1	LIM domain kinase 1	NM_002314	2.44
SERPINF1	Serpin peptidase inhibitor, clade F	NM_002615	2.42
NHLH1	Nescient helix loop helix 1	NM_005598	2.42
STAT3	Signal transducer and activator of transcription 3	NM_003150	2.39
UNC5C	Unc-5 homolog C (C. elegans)	NM_003728	2.36
POU6F1	POU domain, class 6, transcription factor 1	NM_002702	2.35
ACCN1	Amiloride-sensitive cation channel 1,	NM_001094	2.26
CD9	CD9 molecule	NM_001769	2.25
SLIT2	Slit homolog 2 (Drosophila)	NM_004787	2.18
MTSS1	Metastasis suppressor 1	NM_014751	2.11
NDP	Norrie disease (pseudoglioma)	NM_000266	2.01
GSS	Glutathione synthetase	NM_000178	1.86
SPOCK1	Sparc/osteonectin, cwcv and kazal-like domains proteoglycan	NM_004598	1.81
FGF2	Fibroblast growth factor 2 (basic)	NM_002006	1.80
NINJ2	Ninjurin 2	NM_016533	1.78
TFAP2B	Transcription factor AP-2 beta	NM_003221	1.76
NINJ1	Ninjurin 1	NM_004148	1.65
WNT1	Wingless-type MMTV integration site family, member 1	NM_005430	1.64
ARNT2	Aryl-hydrocarbon receptor nuclear translocator 2	NM_014862	1.63
ROBO1	Roundabout, axon guidance receptor, homolog 1 (Drosophila)	NM_002941	1.60

Symbol	Genes name	Ref Seq Number	Fold change
S100B	S100 calcium binding protein B	NM_006272	1.58
PDGFC	Platelet derived growth factor C	NM_016205	1.54

Table 3

Gene expression alteration of hMSCs in scaffold (signal transduction)

Symbol	Gene name	Ref Seq Number	Fold change
GYS1	Glycogen synthase 1 (muscle)	NM_002103	45.14
GADD45A	Growth arrest and DNA-damage-inducible, alpha	NM_001924	38.32
EGFR	Epidermal growth factor receptor	NM_005228	25.68
WISP2	WNT1 inducible signaling pathway protein 2	NM_003881	22.74
NAB2	NGFI-A binding protein 2 (EGR1 binding protein 2)	NM_005967	18.21
ICAM1	Intercellular adhesion molecule 1 (CD54), human rhinovirus receptor	NM_000201	17.70
TMEPAI	Transmembrane, prostate androgen induced RNA	NM_020182	17.17
TCF7	Transcription factor 7 (T-cell specific, HMG-box)	NM_003202	16.83
CSF2	Colony stimulating factor 2 (granulocyte-macrophage)	NM_000758	16.43
TANK	TRAF family member-associated NFKB activator	NM_004180	16.27
CDKN2C	Cyclin-dependent kinase inhibitor 2C (p18, inhibits CDK4)	NM_078626	16.15
NFKB1	Nuclear factor of kappa light polypeptide gene enhancer in B-cells 1	NM_003998	15.51
CDKN2D	Cyclin-dependent kinase inhibitor 2D (p19, inhibits CDK4)	NM_001800	15.38
RBBP8	Retinoblastoma binding protein 8	NM_002894	15.35
NFKBIA	Nuclear factor of kappa light polypeptide gene enhancer in B-cells inhibitor, alpha	NM_020529	14.72
CSN2	Casein beta	NM_001891	13.64
CDX1	Caudal type homeobox transcription factor 1	NM_001804	13.45
JUN	Jun oncogene	NM_002228	12.64
FOS	V-fos FBJ murine osteosarcoma viral oncogene homolog	NM_005252	12.53
PPARG	Peroxisome proliferator-activated receptor gamma	NM_015869	11.71
HSP90AA2	Heat shock protein 90kDa alpha (cytosolic), class A member 2	NM_001040141	11.27
WISP1	WNT1 inducible signaling pathway protein 1	NM_003882	10.94
FASN	Fatty acid synthase	NM_004104	10.42
HK2	Hexokinase 2	NM_000189	9.42
BIRC5	Baculoviral IAP repeat-containing 5 (survivin)	NM_001168	8.45
JUNB	Jun B proto-oncogene	NM_002229	8.11
STRA6	Stimulated by retinoic acid gene 6 homolog	NM_022369	7.01
CTSD	Cathepsin D	NM_001909	6.95
BCL2	B-cell CLL/lymphoma 2	NM_000633	6.15
MYC	V-myc myelocytomatosis viral oncogene homolog (avian)	NM_002467	5.71
BMP4	Bone morphogenetic protein 4	NM_130851	5.56
WNT1	Wingless-type MMTV integration site family, member 1	NM_005430	5.46
CDKN1B	Cyclin-dependent kinase inhibitor 1B (p27, Kip1)	NM_004064	5.32
TFRC	Transferrin receptor (p90, CD71)	NM_003234	5.06
CXCL9	Chemokine (C-X-C motif) ligand 9	NM_002416	4.90
CDKN1C	Cyclin-dependent kinase inhibitor 1C (p57, Kip2)	NM_000076	4.67
CEBPB	CCAAT/enhancer binding protein (C/EBP), beta	NM_005194	4.49
A2M	Alpha-2-macroglobulin	NM_000014	4.25
IL4R	Interleukin 4 receptor	NM_000418	3.78

Symbol	Gene name	Ref Seq Number	Fold change
BRCA1	Breast cancer 1, early onset	NM_007294	3.63
BAX	BCL2-associated X protein	NM_004324	3.59
ATF2	Activating transcription factor 2	NM_001880	3.37
IRF1	Interferon regulatory factor 1	NM_002198	3.36
CDK2	Cyclin-dependent kinase 2	NM_001798	3.07
BMP2	Bone morphogenetic protein 2	NM_001200	3.01
EGR1	Early growth response 1	NM_001964	2.99
BIRC3	Baculoviral IAP repeat-containing 3	NM_001165	2.63
IKBKB	Inhibitor of kappa light polypeptide gene enhancer in B-cells	NM_001556	2.56
CCL2	Chemokine (C-C motif) ligand 2	NM_002982	2.39
EN1	Engrailed homeobox 1	NM_001426	2.19
BIRC2	Baculoviral IAP repeat-containing 2	NM_001166	1.74
CDKN2A	Cyclin-dependent kinase inhibitor 2A	NM_000077	1.63
CDKN2B	Cyclin-dependent kinase inhibitor 2B (p15, inhibits CDK4)	NM_004936	1.58

Table 4

Primer sequences of genes applied in real-time RT-PCR

Gene	Sense	Antisense	Size
sActin	5′CCATCATGAAGTGTGACGTTG	5′CAATGATCTTGATCTTCATGGTG	150bp
MDK	5′CAAGAAAGGGAAGGGAAAGG	5′AGCAGACAGAAGGCACTGGT	131bp
VEGFA	5′AGGCCAGACATAGGAGAGA	5′TTTCTTGCGATTTCGTTTT	135bp
TGFB2	5′CGCCAAGGAGGTTTACAAAA	5′CTCCATTGGATGAGACGTCAA	115bp
NOTCH4	5′CACGTGAACCCATGTGAGTC	5′TCCAGGTTTGGGAGTACAGG	117bp
BCL2	5′GTTGGGCAACAGAGAACCAT	5′TTCTCCTTTTGGGGCTTTTT	193bp
BIRC5	5′ACCTGAAAGCTTCCTCGACA	5′TAACCTGCCATTGGAACCTC	184bp